Land Use Influences Dissolved Organic Matter Composition in the U.S. Coastal Critical Zone Network

Aleksandar I. Goranov[1], Elizabeth V. Whitney[2], Brian R. Moyer[3], Katherine L. Tully[3], Patrick G. Hatcher[1], Yu-Ping Chin[2]

[1]Department of Chemistry and Biochemistry, Old Dominion University, Norfolk, VA 23529
[2]Civil, Construction, and Environmental Engineering, University of Delaware, Newark, DE, 19716
[3]Department of Plant Science & Landscape Architecture, University of Maryland, College Park, MD 20742

Corresponding authors: Drs. Aleksandar Goranov (aleksandar.i.goranov@gmail.com) and Yu-Ping Chin (yochin@udel.edu)

Table of Contents

Section 1. Ultrahigh resolution mass spectrometric analysis

1.1. Tune validation and quality control

The ESI-FT-ICR-MS instrument used here is calibrated daily with a freshly prepared polyethylene glycol (PEG) standard (Goranov et al., 2022; Romson and Emmer, 2021). After achievement of an acceptable tune, Suwannee River Fulvic Acid (SRFA) standard from the International Humic Substances Society (https://humic-substances.org/) was used to validate tune following the recommendations by the recent ESI-FT-MS interlaboratory comparison study (Hawkes et al., 2020). SRFA was analyzed as 20 mg/L carbon-equivalents in 1:1 MeOH:H_2O solution (H_2O = ultrapure laboratory-grade Milli-Q water; MeOH = Fisher Scientific, Optima LC-MS grade). The obtained mass spectrum (Fig. S1) was processed as described in the manuscript. The molecular formulas (Fig. S2) were assessed of their fit within the H/C, O/C, m/z, and modified aromaticity index (AI_{MOD}) ranges recommended by the interlaboratory comparison study (Hawkes et al., 2020).

We determined that the measured SRFA molecular composition fit all molecular ranges (H/C, O/C, MW, AI_{MOD} listed in Table S1) indicating that the tune was appropriately set for sequential analyses of natural organic matter. The acquired data would be comparable with previously published datasets as well as such that will be published in the future using the ESI-FT-MS interlaboratory comparison study recommendations (Hawkes et al., 2020). Notably, only 86 % of the commonly measured peaks from the ESI-FT-MS interlaboratory comparison study (Hawkes et al., 2020) were detected by our instrument, which is lower than the recommended threshold (95 %). This was likely due to the poorly functioning quadrupole sector analyzer of our instrument. Due to its age, it is unable to properly select ions at a broad range limiting the detected ions to 300-700 m/z and omitting commonly detected species in the 200-300 and 700-900 m/z ranges.

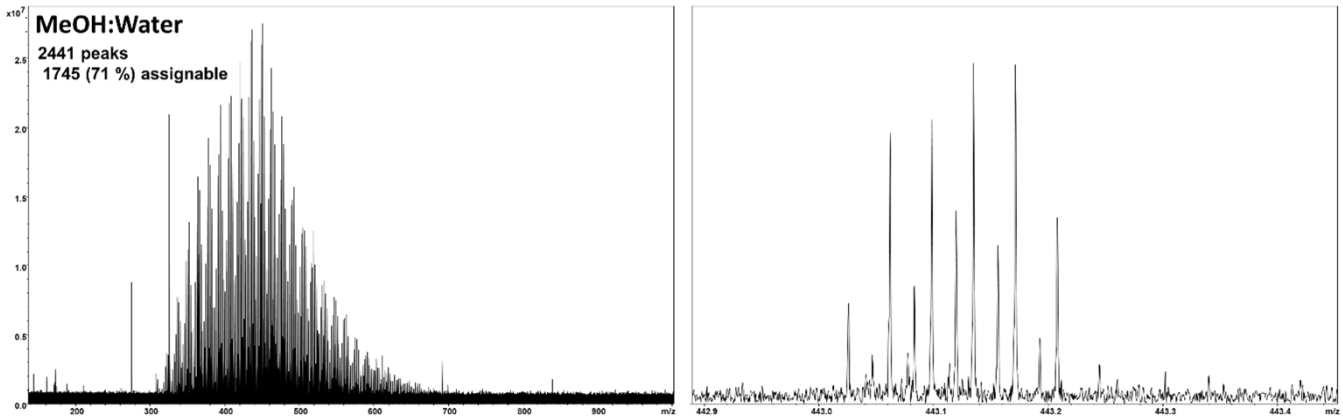

Figure S1. Whole (-)ESI-FT-ICR mass spectrum (left) and an expanded window at nominal mass of 443 (right) for Suwannee River Fulvic Acid standard reference material in MeOH:Water solvent conditions.

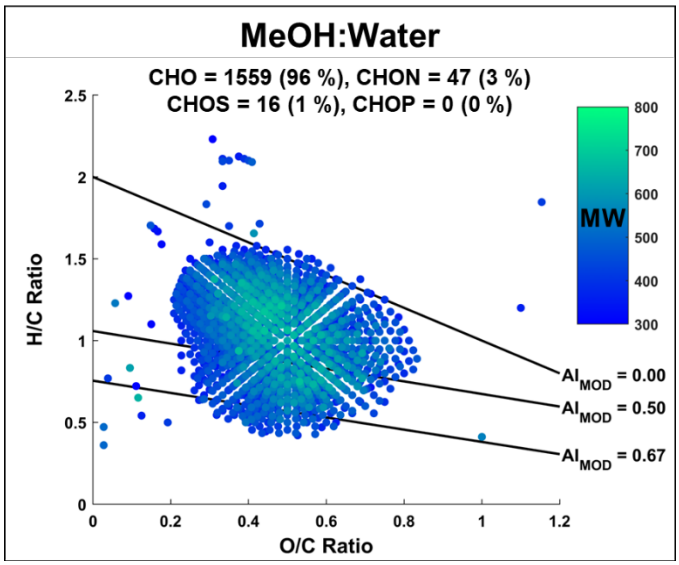

Figure S2. Van Krevelen diagram (H/C versus O/C molar ratio plot) of assigned molecular formulas to Suwannee River Fulvic Acid standard reference material prepared in MeOH:Water solvent conditions. Formulas are color-coded based on their molecular weight (MW). The black lines indicate modified aromaticity index cutoffs (AI_{MOD})(Koch and Dittmar, 2006, 2016).

Table S1. Comparison of tune validation parameters of a quality control Suwannee River Fulvic Acid (SRFA) spectrum relative to recommended criteria by the ESI-FT-MS interlaboratory comparison study (Hawkes et al., 2020). AI_{MOD} = modified aromaticity index.

Parameter	Recommendation by Hawkes et al. (2020)	Quality control SRFA spectrum
Detected common ions	≥ 95 %	87 %
Intensity-weighed H/C	1.09 ± 0.04	1.16
Intensity-weighed O/C	0.52 ± 0.03	0.48
Intensity-weighed AI_{MOD}	0.34 ± 0.02	0.33
Intensity-weighed m/z	423 ± 46 Da	451

1.2. Optimization of sample preparation conditions

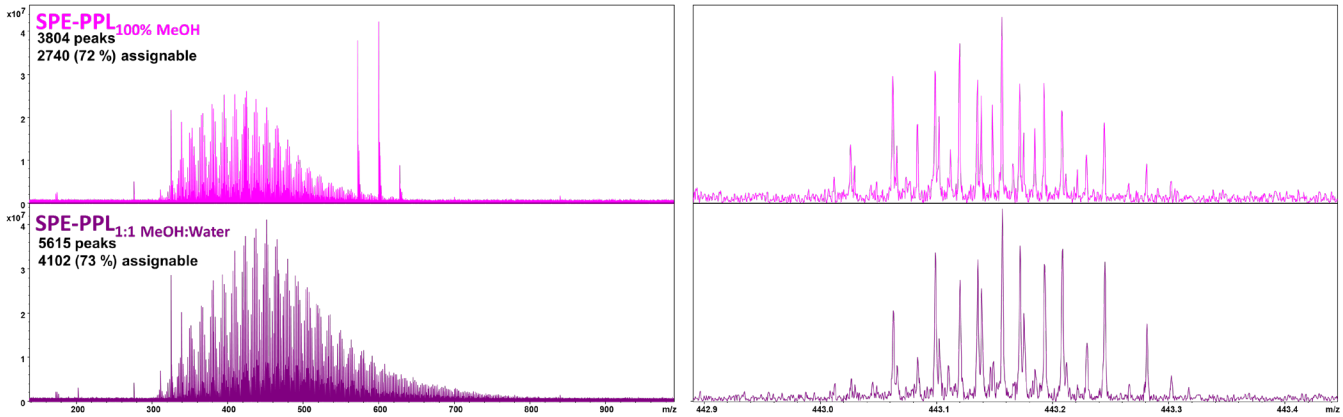

Figure S3. Whole (-)ESI-FT-ICR mass spectra (left) and expanded windows at nominal mass of 443 (right) for VA Farm DOM sample prepared using the **SPE-PPL100% MeOH** and **SPE-PPL1:1 MeOH:Water** sample preparation techniques (Goranov et al. 2022).

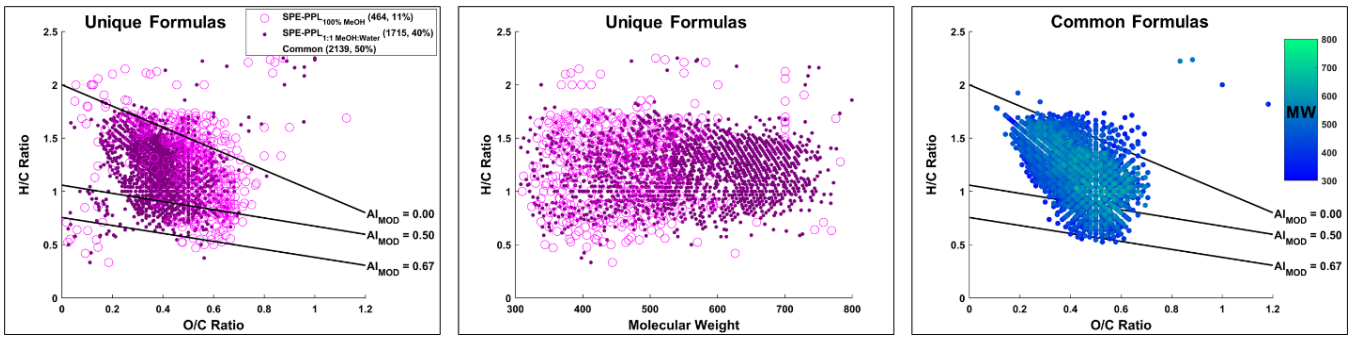

Figure S4. Presence/absence analysis (Sleighter et al., 2012) on VA Farm DOM molecular compositions obtained following **SPE-PPL100% MeOH** and **SPE-PPL1:1 MeOH:Water** sample preparation techniques (Goranov et al. 2022). Van Krevelen diagram (H/C versus O/C molar ratio plots) of the unique formulas (present only in the composition from one of the approaches) is shown on the left panel, H/C versus molecular weight (MW) plot of unique formulas is shown in the middle panel, and the van Krevelen diagram on the right shows the common formulas of the two samples being compared (color-coded based on MW). The number of unique and common formulas is listed in the legends along with corresponding percentages (relative to total number of formulas in the two samples being compared). The black lines indicate modified aromaticity index cutoffs (AI_{MOD}) (Koch and Dittmar, 2006, 2016).

Section 2. Formula categorization into compound classes

Molecular formulas can be classified into different molecular categories referred to as "compound classes". These groups are exclusive (i.e., compound classes do not overlap) and therefore this is a crude approach to classify observed molecular formulas based on assumed structure and biopolymeric source. This approach of separating the van Krevelen space into succinct regions has been useful in studying DOM biogeochemistry in various systems (Antony et al., 2017; He et al., 2019; He et al., 2018; Hockaday et al., 2009; Ikeya et al., 2015; Kim et al., 2003; Koch et al., 2005; Kujawinski and Behn, 2006; Ohno et al., 2010; Ohno et al., 2014; Ohno et al., 2016, 2018; Santl-Temkiv et al., 2013; Schmidt et al., 2009; Sleighter et al., 2015; Sleighter et al., 2014). However, compound class assignments to formulas are not unambiguous, which is an issue that has been discussed in detail by Sleighter and Hatcher (2008). Fundamentally, the reason for this is the high number of structural isomers that are possible for molecular formulas (Hertkorn et al., 2007; Wieland et al., 1996).

Table S2. Stoichiometric boundaries used to define five compound classes for coastal dissolved organic matter categorization. DBE = double-bond equivalency; AI_{MOD} = modified aromaticity index.

Compound Class	Stoichiometric Boundaries	Reference
Carboxyl-rich Alicyclic Molecules (CRAM)	$0.30 \leq DBE/C \leq 0.68$ $0.20 \leq DBE/H \leq 0.95$ $0.77 \leq DBE/O \leq 1.75$	Hertkorn et al. (2006)
Lignin	$AI_{MOD} < 0.67$ $H/C < 1.5$ $0.1 < O/C < 0.67$	Goranov et al. (2023)
Lipid (includes saturated aliphatics)	$1.5 \leq H/C < 2$ $O/C < 0.67$ $N = 0$	Goranov et al. (2023)
Condensed Aromatic Compounds (ConAC)	$AI_{MOD} \geq 0.67$	Koch and Dittmar (2006); Koch and Dittmar (2016)
Tannin	$AI_{MOD} < 0.67$ $H/C < 1.5$ $O/C \geq 0.67$	Goranov et al. (2023)
Others	Formulas that do not fit in any of the boundaries above	

Table S3. Compound class categorization of molecular formulas.

	CRAM	Lignin	Lipid	Condensed Aromatics	Tannin	Others
VA Forest	1656 (65 %)	587 (23 %)	138 (5 %)	129 (5 %)	19 (1 %)	10 (0 %)
VA Farm	2606 (68 %)	615 (16 %)	528 (14 %)	34 (1 %)	14 (0 %)	57 (1 %)
DE Forest	2540 (67 %)	799 (21 %)	244 (6 %)	131 (3 %)	51 (1 %)	32 (1 %)
DE Farm	2636 (68 %)	754 (20 %)	277 (7 %)	87 (2 %)	65 (2 %)	38 (1 %)
MD Forest	2455 (65 %)	827 (22 %)	247 (7 %)	152 (4 %)	56 (1 %)	56 (1 %)
MD Farm	2484 (68 %)	747 (20 %)	264 (7 %)	89 (2 %)	35 (1 %)	45 (1 %)

Section 3. Molecular weight distributions of assigned molecular formulas

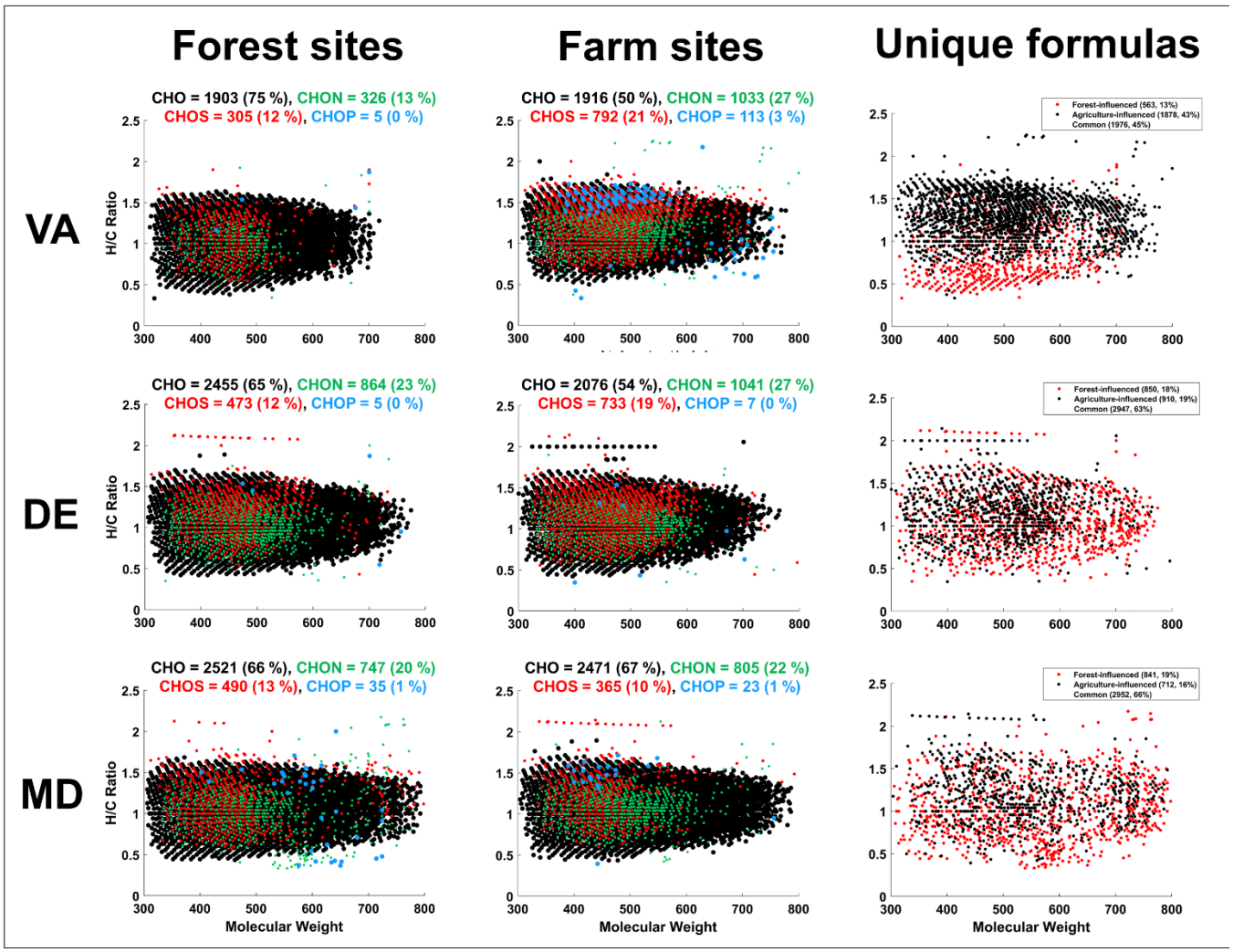

Figure S5. H/C versus Molecular Weight plots of formulas found in coastal dissolved organic matter (DOM) under forested (left panels) and agricultural influence (middle panels) in Virginia (top panels), Delaware (middle panels), and Maryland (bottom panels), with formulas color coded based on type of molecular formulas (CHO in **black**, CHON in **green**, CHOS in **red**, and CHOP in **blue**). Presence-absence analysis (Sleighter et al., 2012) was used to identify formulas that are only found in the forest-influenced or farm-influenced DOM samples (colored in **red** and **black**, respectively, on the right panels). Number of formulas and corresponding percentages (relative to total number of formulas) are shown in the legends for the respective formula pools.

Section 4. Presence-absence analysis of molecular data

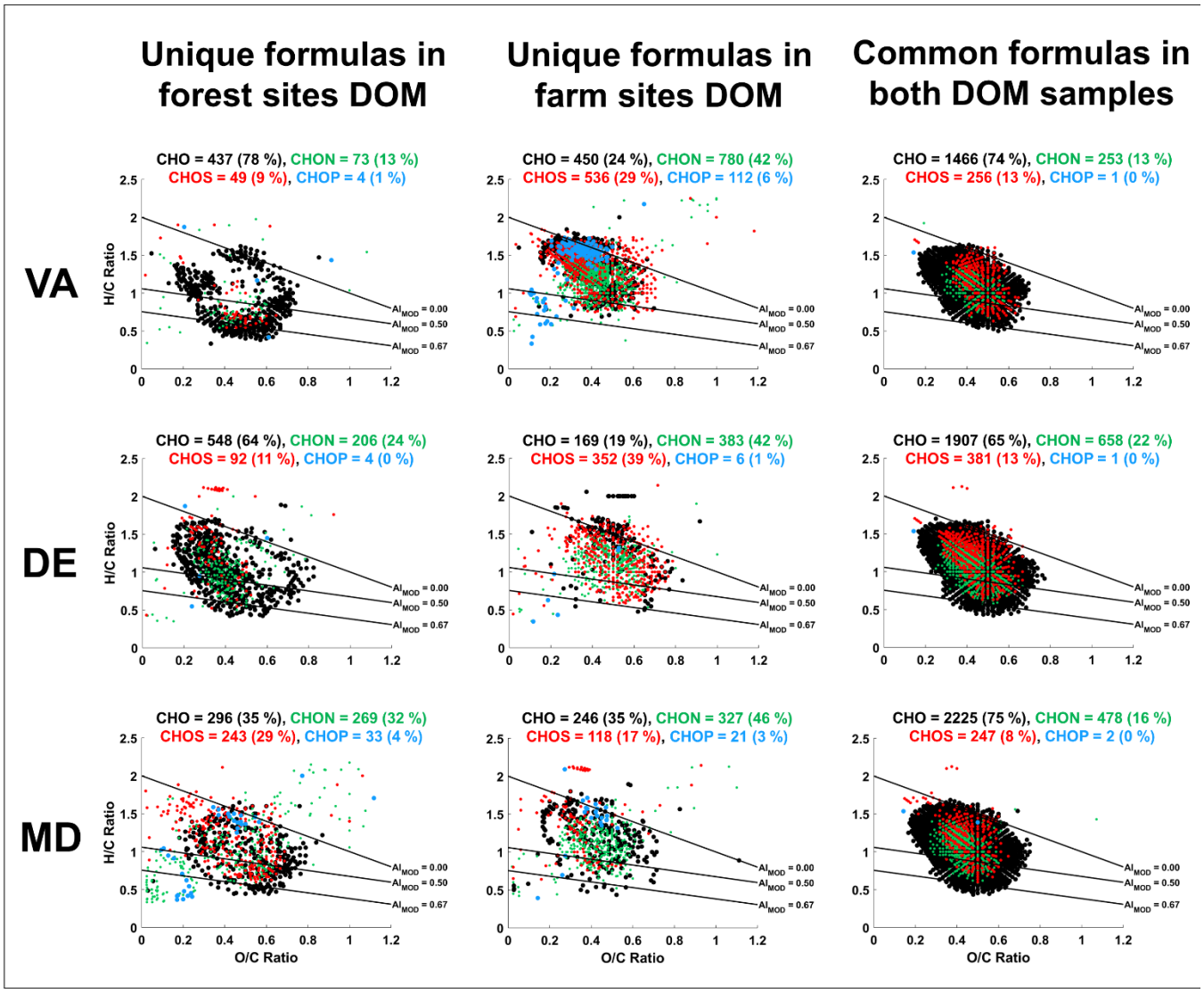

Figure S6. Presence-absence analysis (Sleighter et al., 2012) of coastal dissolved organic matter (DOM) under forested and agricultural influence. Molecular formulas are color-coded based on type of molecular formulas (CHO in **black**, CHON in **green**, CHOS in **red**, and CHOP in **blue**). Number of formulas and corresponding percentages (relative to total number of formulas) are shown in the legends for the respective formula pools. Black lines separate the van Krevelen diagrams based on modified aromaticity index (AI_{MOD}) (Koch and Dittmar, 2006, 2016).

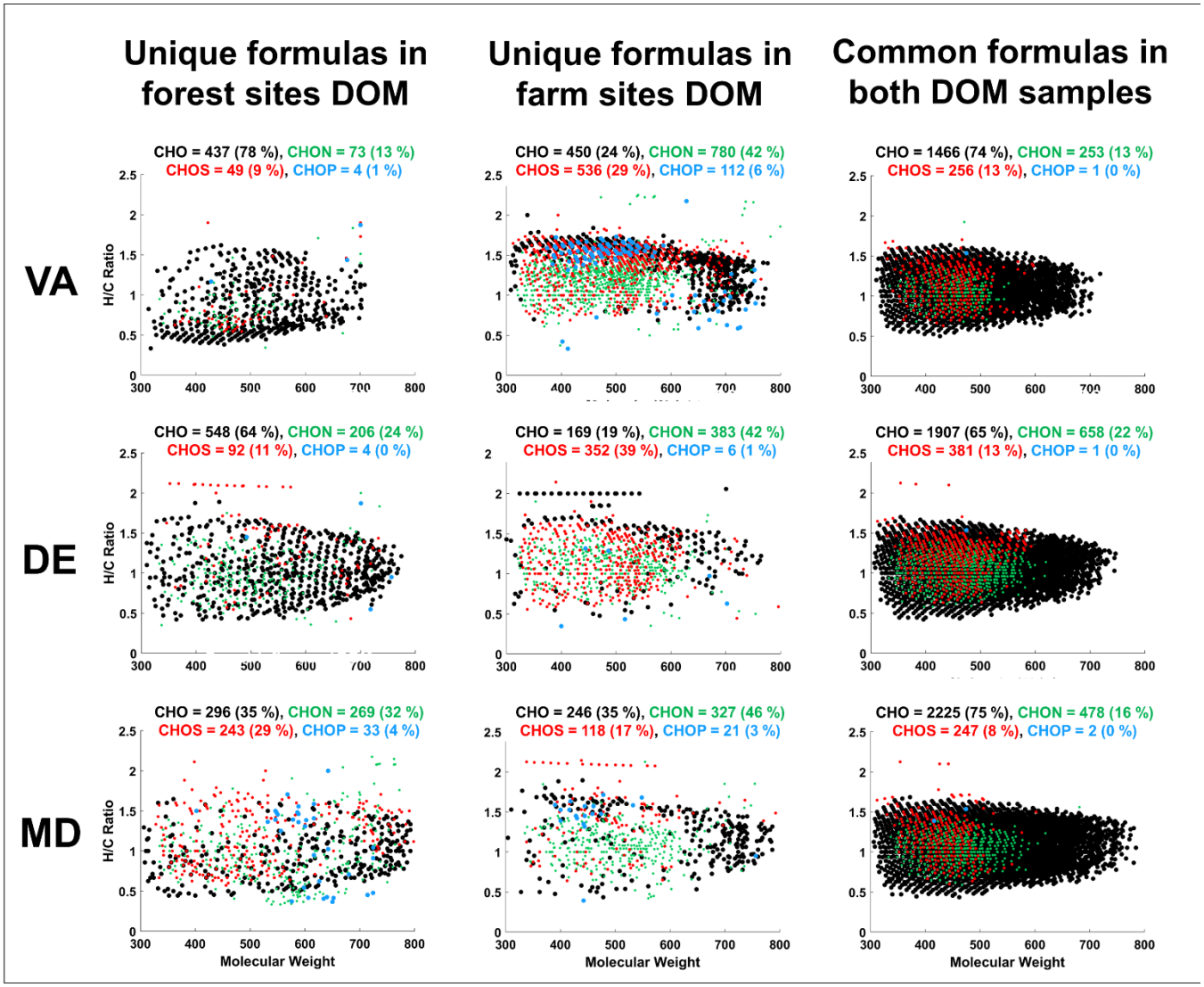

Figure S7. Presence-absence analysis (Sleighter et al., 2012) of coastal dissolved organic matter (DOM) under forested and agricultural influence. Molecular formulas are color-coded based on type of molecular formulas (CHO in **black**, CHON in **green**, CHOS in **red**, and CHOP in **blue**). Number of formulas and corresponding percentages (relative to total number of formulas) are shown in the legends for the respective formula pools.

Section 5. Kendrick mass defect exploration of molecular data

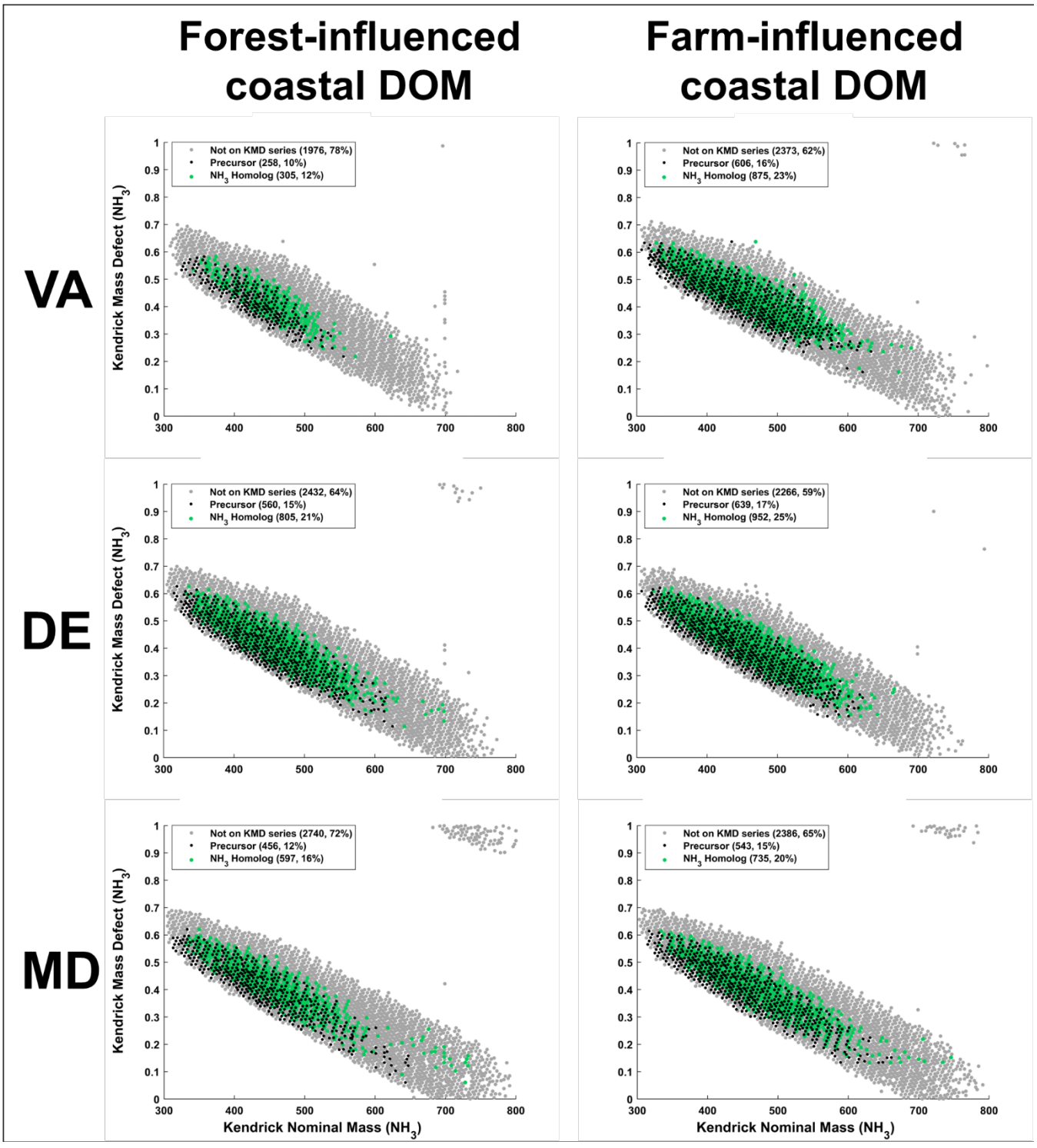

Figure S8. Kendrick mass defect analysis of molecular formula catalogs that seeks formulas that differ by 17.026549 Da (mass of NH_3). Precursor formulas (first formula on a series) are typically CHO formulas color-coded in **black**, NH_3 homologs are color-coded in **green**, formulas not on KMD series are color-coded in **gray**. Corresponding molecular formulas are plotted on van Krevelen plots on Figure S9.

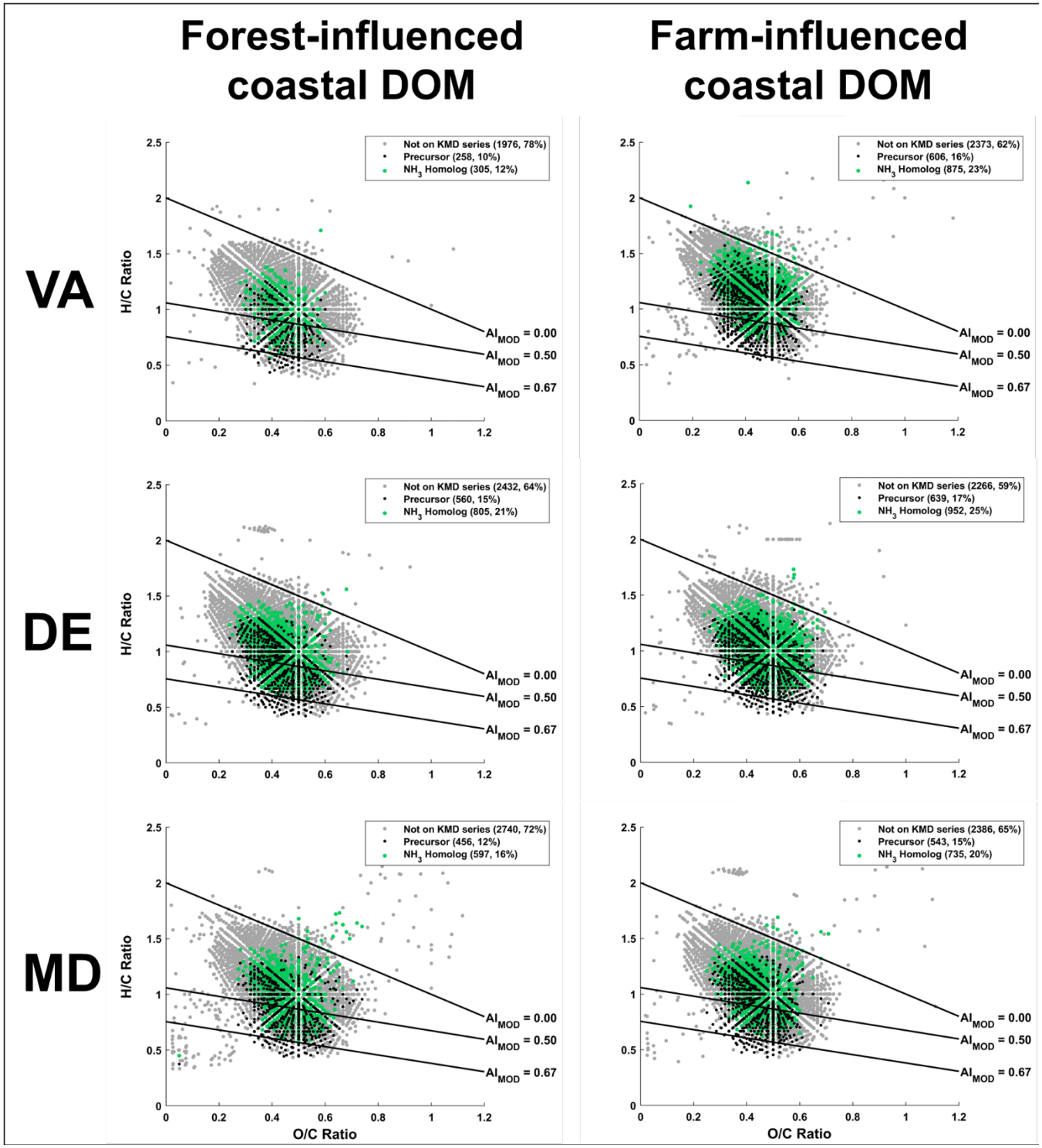

Figure S9. Van Krevelen diagrams of molecular formulas categorized by Kendrick mass defect analysis for NH_3 homologs. Precursor formulas (first formula on a series) are typically CHO formulas color-coded in **black**, NH_3 homologs are color-coded in **green**, formulas not on KMD series are color-coded in **gray**.

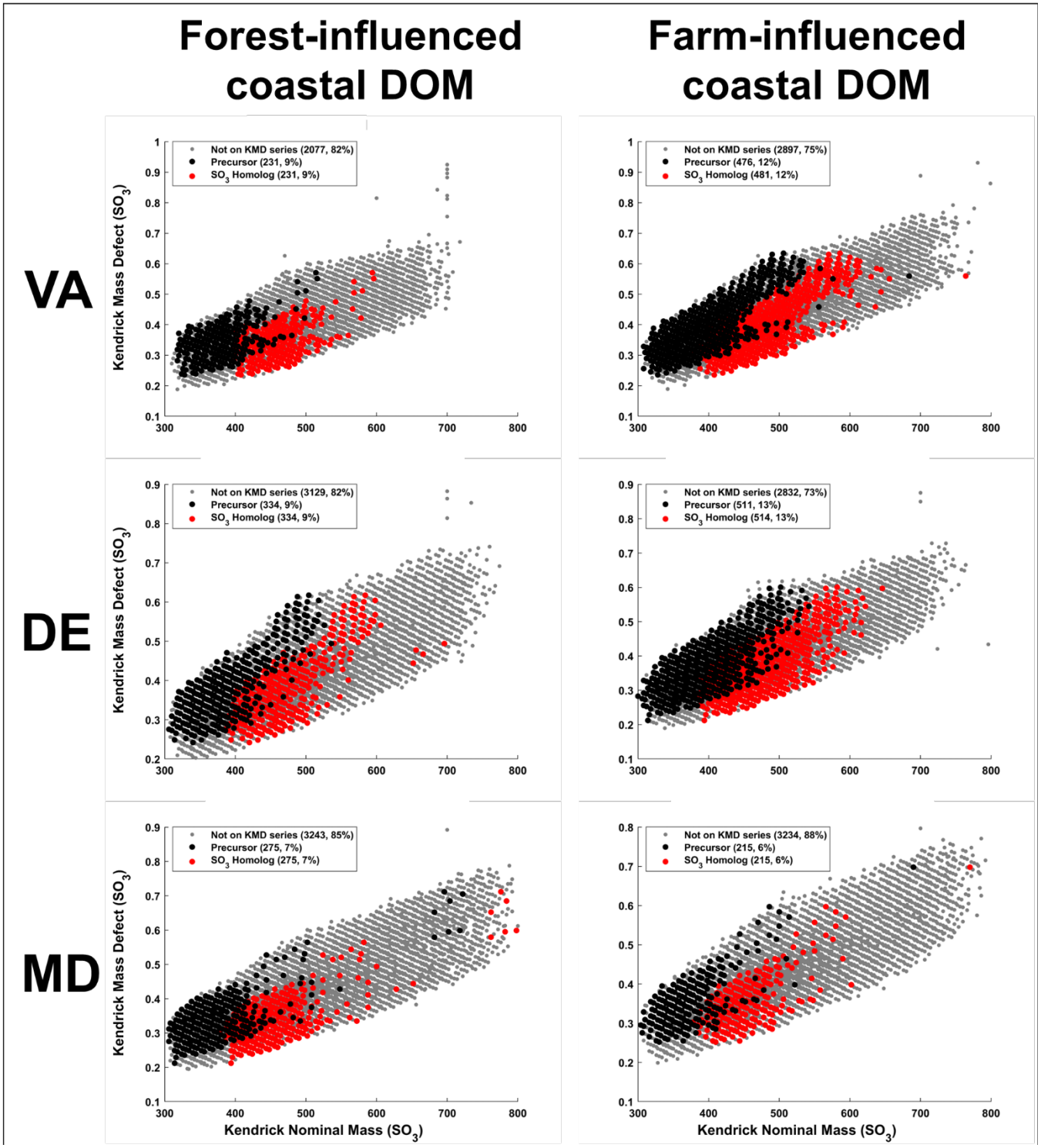

Figure S10. Kendrick mass defect analysis of molecular formula catalogs that seeks formulas that differ by 79.956815 Da (mass of SO_3). Precursor formulas (first formula on a series) are typically CHO formulas color-coded in **black**, SO_3 homologs are color-coded in **red**, formulas not on KMD series are color-coded in **gray**. Corresponding molecular formulas are plotted on van Krevelen plots on Figure S11.

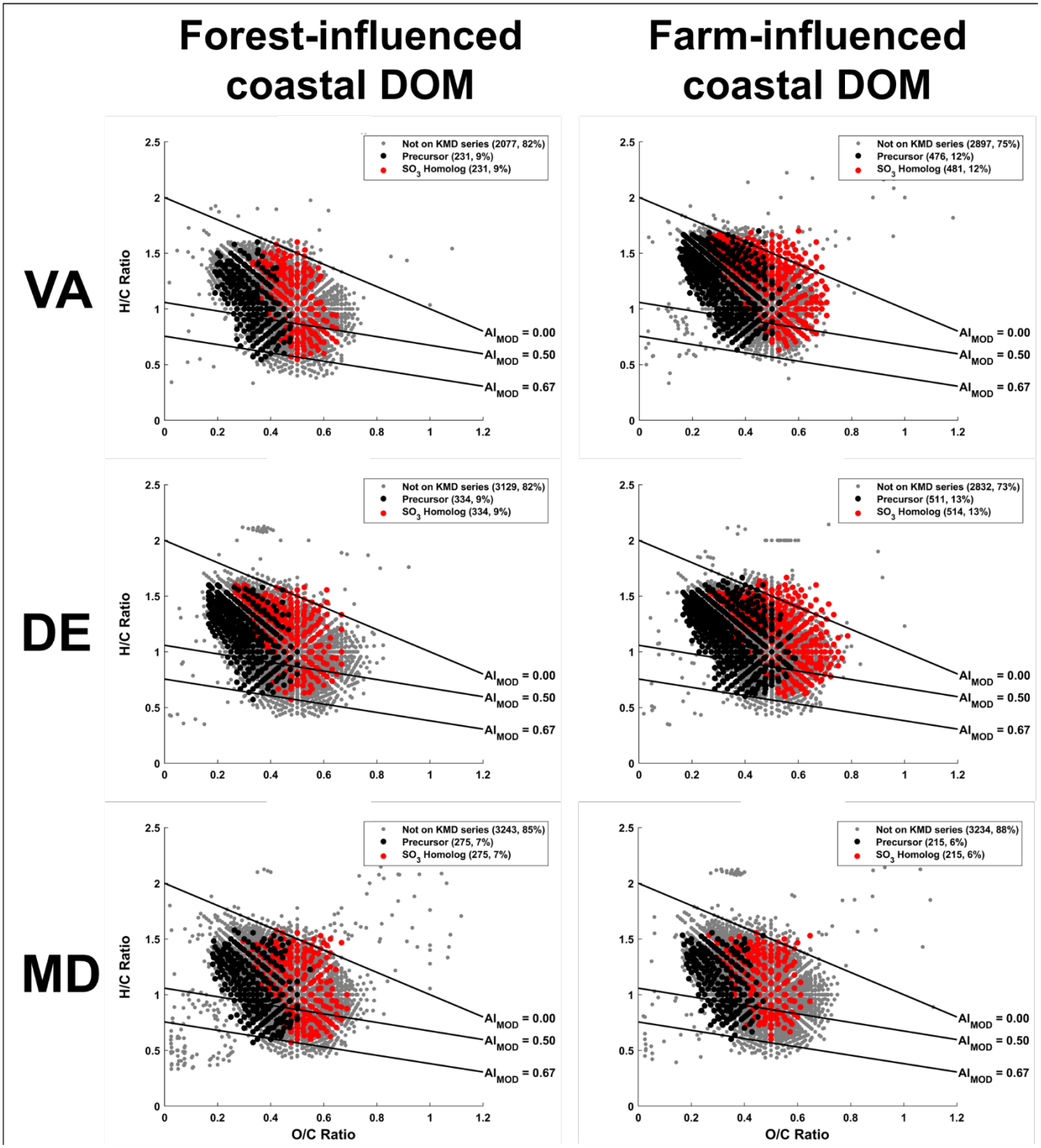

Figure S11. Van Krevelen diagrams of molecular formulas categorized by Kendrick mass defect analysis for SO_3 homologs. Precursor formulas (first formula on a series) are typically CHO formulas color-coded in **black**, SO_3 homologs are color-coded in **red**, formulas not on KMD series are color-coded in **gray**.

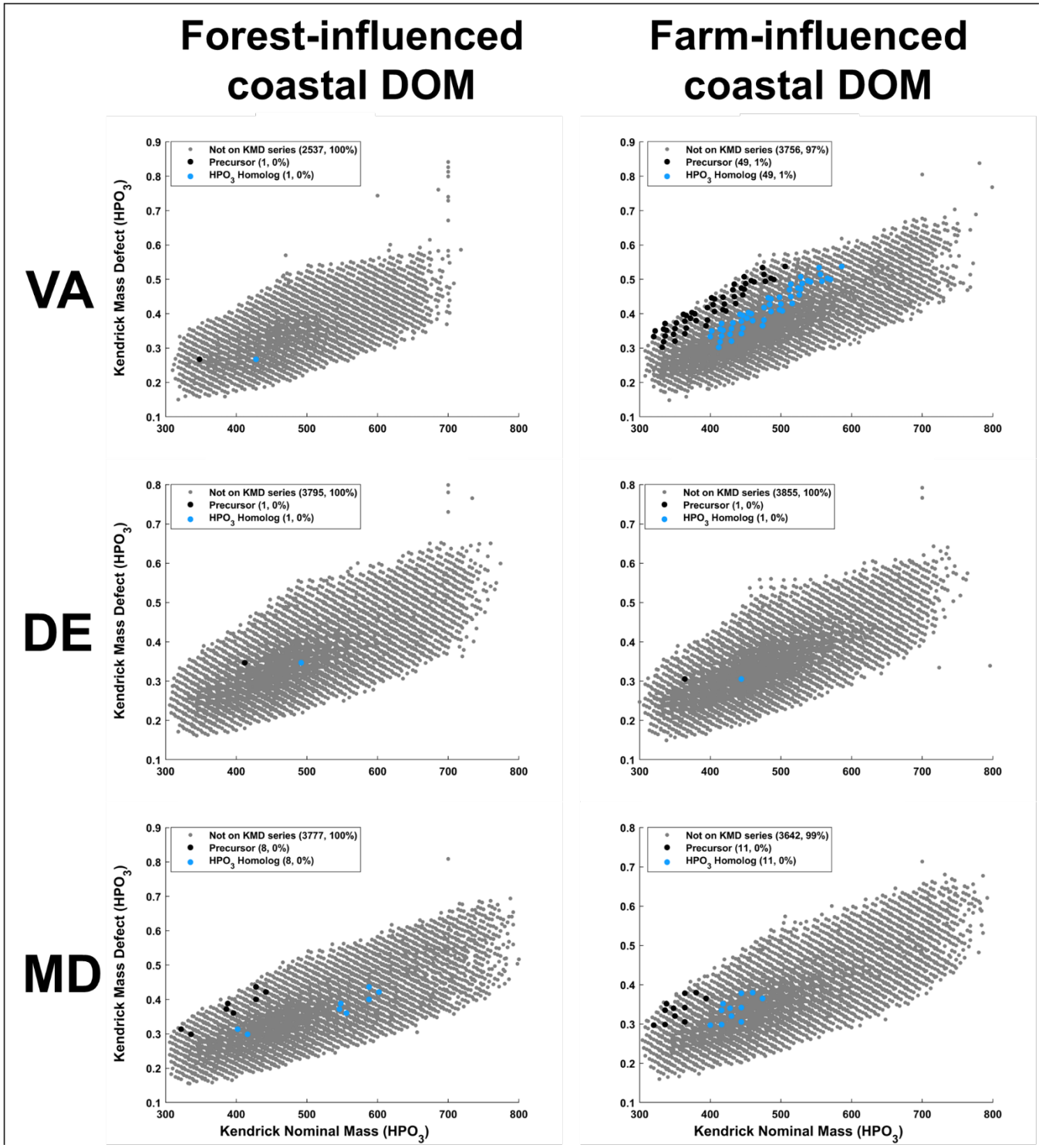

Figure S12. Kendrick mass defect analysis of molecular formula catalogs that seeks formulas that differ by 79.966330 Da (mass of HPO_3). Precursor formulas (first formula on a series) are typically CHO formulas color-coded in **black**, HPO_3 homologs are color-coded in **blue**, formulas not on KMD series are color-coded in **gray**. Corresponding molecular formulas are plotted on van Krevelen plots on Figure S13.

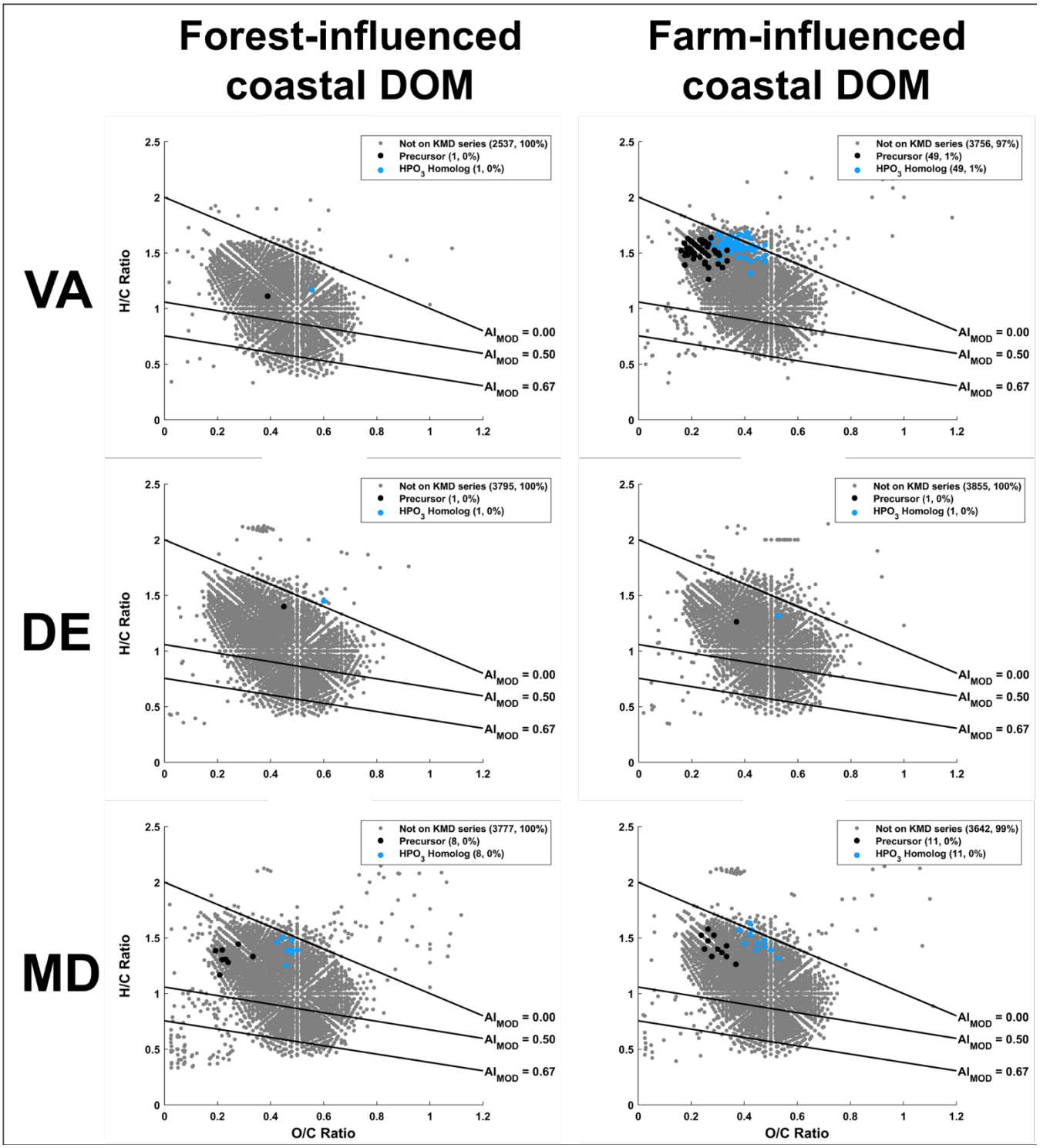

Figure S13. Van Krevelen diagrams of molecular formulas categorized by Kendrick mass defect analysis for HPO_3 homologs. Precursor formulas (first formula on a series) are typically CHO formulas color-coded in **black**, HPO_3 homologs are color-coded in **blue**, formulas not on KMD series are color-coded in **gray**.

References

Antony, R., Willoughby, A.S., Grannas, A.M., Catanzano, V., Sleighter, R.L., Thamban, M., Hatcher, P.G., Nair, S., 2017. Molecular insights on dissolved organic matter transformation by supraglacial microbial communities. Environmental science & technology 51(8), 4328-4337. doi.org/10.1021/acs.est.6b05780.

Goranov, A.I., Sleighter, R.L., Yordanov, D.A., Hatcher, P., 2023. TEnvR: MATLAB-based toolbox for environmental research. Analytical Methods(15), 5390-5400. doi.org/10.1039/D3AY00750B.

Goranov, A.I., Tadini, A.M., Martin-Neto, L., Bernardi, A.C.C., Oliveira, P.P.A., Pezzopane, J.R.M., Milori, D., Mounier, S., Hatcher, P.G., 2022. Comparison of sample preparation techniques for the (-)ESI-FT-ICR-MS analysis of humic and fulvic acids. Environmental science & technology 56(17), 12688-12701. doi.org/10.1021/acs.est.2c01125.

Hawkes, J.A., D'Andrilli, J., Agar, J.N., Barrow, M.P., Berg, S.M., Catalán, N., Chen, H., Chu, R.K., Cole, R.B., Dittmar, T., Gavard, R., Gleixner, G., Hatcher, P.G., He, C., Hess, N.J., Hutchins, R.H.S., Ijaz, A., Jones, H.E., Kew, W., Khaksari, M., Palacio Lozano, D.C., Lv, J., Mazzoleni, L.R., Noriega-Ortega, B.E., Osterholz, H., Radoman, N., Remucal, C.K., Schmitt, N.D., Schum, S.K., Shi, Q., Simon, C., Singer, G., Sleighter, R.L., Stubbins, A., Thomas, M.J., Tolic, N., Zhang, S., Zito, P., Podgorski, D.C., 2020. An international laboratory comparison of dissolved organic matter composition by high resolution mass spectrometry: Are we getting the same answer? Limnology and Oceanography: Methods 18(6), 235-258. doi.org/10.1002/lom3.10364.

He, Z., Sleighter, R.L., Hatcher, P.G., Liu, S., Wu, F., Zou, H., Olanya, O.M., 2019. Molecular level comparison of water extractives of maple and oak with negative and positive ion ESI FT-ICR mass spectrometry. Journal of Mass Spectrometry 54(8), 655-666. doi.org/10.1002/jms.4379.

He, Z.Q., Guo, M.X., Sleighter, R.L., Zhang, H.L., Chanel, F., Hatcher, P.G., 2018. Characterization of defatted cottonseed meal-derived pyrolysis bio-oil by ultrahigh resolution electrospray ionization Fourier transform ion cyclotron resonance mass spectrometry. Journal of Analytical and Applied Pyrolysis 136, 96-106. doi.org/10.1016/j.jaap.2018.10.018.

Hertkorn, N., Benner, R., Frommberger, M., Schmitt-Kopplin, P., Witt, M., Kaiser, K., Kettrup, A., Hedges, J.I., 2006. Characterization of a major refractory component of marine dissolved organic matter. Geochimica et Cosmochimica Acta 70(12), 2990-3010. doi.org/10.1016/j.gca.2006.03.021.

Hertkorn, N., Ruecker, C., Meringer, M., Gugisch, R., Frommberger, M., Perdue, E.M., Witt, M., Schmitt-Kopplin, P., 2007. High-precision frequency measurements: Indispensable tools at the core of the molecular-level analysis of complex systems. Analytical and Bioanalytical Chemistry 389(5), 1311-1327. doi.org/10.1007/s00216-007-1577-4.

Hockaday, W.C., Purcell, J.M., Marshall, A.G., Baldock, J.A., Hatcher, P.G., 2009. Electrospray and photoionization mass spectrometry for the characterization of organic matter in natural waters: A qualitative assessment. Limnology and Oceanography: Methods 7, 81-95. doi.org/10.4319/lom.2009.7.81.

Ikeya, K., Sleighter, R.L., Hatcher, P.G., Watanabe, A., 2015. Characterization of the chemical composition of soil humic acids using Fourier transform ion cyclotron resonance mass spectrometry. Geochimica et Cosmochimica Acta 153, 169-182. doi.org/10.1016/j.gca.2015.01.002.

Kim, S., Kramer, R.W., Hatcher, P.G., 2003. Graphical method for analysis of ultrahigh-resolution broadband mass spectra of natural organic matter, the van Krevelen diagram. Analytical chemistry 75(20), 5336-5344. doi.org/10.1021/ac034415p.

Koch, B.P., Dittmar, T., 2006. From mass to structure: an aromaticity index for high-resolution mass data of natural organic matter. Rapid Communications in Mass Spectrometry 20(5), 926-932. doi.org/10.1002/rcm.2386.

Koch, B.P., Dittmar, T., 2016. From mass to structure: an aromaticity index for high-resolution mass data of natural organic matter (Erratum). Rapid Communications in Mass Spectrometry 30(1), 250-250. doi.org/10.1002/rcm.7433.

Koch, B.P., Witt, M.R., Engbrodt, R., Dittmar, T., Kattner, G., 2005. Molecular formulae of marine and terrigenous dissolved organic matter detected by electrospray ionization Fourier transform ion cyclotron resonance mass spectrometry. Geochimica et Cosmochimica Acta 69(13), 3299-3308. doi.org/10.1016/j.gca.2005.02.027.

Kujawinski, E.B., Behn, M.D., 2006. Automated analysis of electrospray ionization Fourier transform ion cyclotron resonance mass spectra of natural organic matter. Analytical chemistry 78(13), 4363-4373. doi.org/10.1021/ac0600306.

Ohno, T., He, Z., Sleighter, R.L., Honeycutt, C.W., Hatcher, P.G., 2010. Ultrahigh resolution mass spectrometry and indicator species analysis to identify marker components of soil- and plant biomass- derived organic matter fractions. Environmental science & technology 44(22), 8594-8600. doi.org/10.1021/es101089t.

Ohno, T., Parr, T.B., Gruselle, M.C., Fernandez, I.J., Sleighter, R.L., Hatcher, P.G., 2014. Molecular composition and biodegradability of soil organic matter: a case study comparing two new England forest types. Environmental science & technology 48(13), 7229-7236. doi.org/10.1021/es405570c.

Ohno, T., Sleighter, R.L., Hatcher, P.G., 2016. Comparative study of organic matter chemical characterization using negative and positive mode electrospray ionization ultrahigh-resolution mass spectrometry. Analytical and Bioanalytical Chemistry 408(10), 2497-2504. doi.org/10.1007/s00216-016-9346-x.

Ohno, T., Sleighter, R.L., Hatcher, P.G., 2018. Adsorptive fractionation of corn, wheat, and soybean crop residue derived water-extractable organic matter on iron (oxy)hydroxide. Geoderma 326, 156-163. doi.org/10.1016/j.geoderma.2018.04.006.

Romson, J., Emmer, A., 2021. Mass calibration options for accurate electrospray ionization mass spectrometry. International Journal of Mass Spectrometry 467, 1-23. doi.org/10.1016/j.ijms.2021.116619.

Santl-Temkiv, T., Finster, K., Dittmar, T., Hansen, B.M., Thyrhaug, R., Nielsen, N.W., Karlson, U.G., 2013. Hailstones: A window into the microbial and chemical inventory of a storm cloud. PloS one 8(1), e53550. doi.org/10.1371/journal.pone.0053550.

Schmidt, F., Elvert, M., Koch, B.P., Witt, M., Hinrichs, K.U., 2009. Molecular characterization of dissolved organic matter in pore water of continental shelf sediments. Geochimica et Cosmochimica Acta 73(11), 3337-3358. doi.org/10.1016/j.gca.2009.03.008.

Sleighter, R.L., Caricasole, P., Richards, K.M., Hanson, T., Hatcher, P.G., 2015. Characterization of terrestrial dissolved organic matter fractionated by pH and polarity and their biological effects on plant growth. Chemical and Biological Technologies in Agriculture 2(1), 1-19. doi.org/10.1186/s40538-015-0036-2.

Sleighter, R.L., Chen, H., Wozniak, A.S., Willoughby, A.S., Caricasole, P., Hatcher, P.G., 2012. Establishing a measure of reproducibility of ultrahigh-resolution mass spectra for complex mixtures of natural organic matter. Analytical chemistry 84(21), 9184-9191. doi.org/10.1021/ac3018026.

Sleighter, R.L., Cory, R.M., Kaplan, L.A., Abdulla, H.A.N., Hatcher, P.G., 2014. A coupled geochemical and biogeochemical approach to characterize the bioreactivity of dissolved organic matter from a headwater stream. Journal of Geophysical Research: Biogeosciences 119(8), 1520-1537. doi.org/10.1002/2013jg002600.

Sleighter, R.L., Hatcher, P.G., 2008. Molecular characterization of dissolved organic matter (DOM) along a river to ocean transect of the lower Chesapeake Bay by ultrahigh resolution electrospray ionization Fourier transform ion cyclotron resonance mass spectrometry. Marine Chemistry 110(3-4), 140-152. doi.org/10.1016/j.marchem.2008.04.008.

Wieland, T., Kerber, A., Laue, R., 1996. Principles of the generation of constitutional and configurational isomers. Journal of Chemical Information and Computer Sciences 36(3), 413-419. doi.org/10.1021/ci9502663.